THE SYNCHROTRON SPECTRUM OF FAST COOLING ELECTRONS REVISITED

JONATHAN GRANOT,[1] TSVI PIRAN,[1] AND RE'EM SARI[2]

ABSTRACT

We discuss the spectrum arising from synchrotron emission by fast cooling (FC) electrons, when fresh electrons are continually accelerated by a strong blast wave, into a power-law distribution of energies. The FC spectrum has so far been described by four power-law segments divided by three break frequencies $\nu_{sa} < \nu_c < \nu_m$. This is valid for a homogeneous electron distribution. However, hot electrons are located right after the shock, while most electrons are farther downstream and have cooled. This spatial distribution changes the optically thick part of the spectrum, introducing a new break frequency, $\nu_{ac} < \nu_{sa}$, and a new spectral slope, $F_\nu \propto \nu^{11/8}$ for $\nu_{ac} < \nu < \nu_{sa}$. The familiar $F_\nu \propto \nu^2$ holds only for $\nu < \nu_{ac}$. This ordering of the break frequencies is relevant for typical gamma-ray burst (GRB) afterglows in an interstellar medium environment. Other possibilities arise for internal shocks or afterglows in dense circumstellar winds. We discuss the possible implications of this spectrum for GRBs and their afterglows in the context of the internal-external shock model. Observations of $F_\nu \propto \nu^{11/8}$ would enable us to probe scales much smaller than the typical size of the system and to constrain the amount of turbulent mixing behind the shock.

Subject headings: gamma rays: bursts — radiation mechanisms: nonthermal — shock waves — turbulence

1. INTRODUCTION

The spectrum of gamma-ray bursts (GRBs) and their afterglows is well described by synchrotron and inverse Compton emission. It is better studied during the afterglow stage, where we have broadband observations. The observed behavior is in good agreement with the theory. Within the fireball model, both the GRB and its afterglow are due to the deceleration of a relativistic flow. The radiation is emitted by relativistic electrons within the shocked regions. According to the internal-external shock scenario, it has been shown by Fenimore et al. (1996) and Sari & Piran (1997) that in order to obtain a reasonable efficiency, the GRB itself must arise from internal shocks (ISs) within the flow, while the afterglow is due to the external shock (ES) produced as the flow is decelerated upon collision with the ambient medium. In the simplest version of the fireball model, a spherical blast wave expands into a cold and homogeneous ambient medium (Waxman 1997; Mészáros & Rees 1997; Katz & Piran 1997; Sari, Piran, & Narayan 1998, hereafter SPN). An important variation is a density profile $\rho(r) \propto r^{-2}$, which is suitable for a massive star progenitor surrounded by its preexplosion wind.

In this Letter, we consider fast cooling (FC), in which the electrons cool because of radiation losses on a timescale much shorter than the dynamical time of the system,[3] t_{dyn}. Both the highly variable temporal structure of most bursts and the requirement of a reasonable radiative efficiency suggest FC during the GRB itself (Sari, Narayan, & Piran 1996). During the afterglow, FC lasts ~1 hr after the burst for an interstellar medium (ISM) surrounding (SPN; Granot, Piran, & Sari 1999a) and ~1 day in a dense circumstellar wind environment (Chevalier & Li 2000). We assume that the electrons (initially) and the magnetic field (always) hold fractions ϵ_e and ϵ_B of the internal energy, respectively. We consider synchrotron emission of relativistic electrons that are accelerated by a strong blast wave into a power-law energy distribution:[4] $N(\gamma) \propto \gamma^{-p}$ for $\gamma \geq \gamma_m = (p-2)\epsilon_e e'/(p-1)n'm_e c^2 \cong \epsilon_e e'/3n'm_e c^2$, where n' and e' are the number density and internal energy density in the local frame, respectively, and we have used the standard value $p = 2.5$.

After being accelerated by the shock, the electrons cool because of synchrotron radiation losses. An electron with a critical Lorentz factor γ_c cools on the dynamical time t_{dyn}:

$$\gamma_c = \frac{6\pi m_e c}{\sigma_T \Gamma B'^2 t_{dyn}} = \frac{3m_e c}{4\sigma_T \Gamma \epsilon_B e' t_{dyn}}, \qquad (1)$$

where Γ is the bulk Lorentz factor, σ_T is the Thomson cross section, and B' is the magnetic field. The Lorentz factors γ_m and γ_c correspond to the frequencies ν_m and ν_c, respectively, using $\nu_{syn}(\gamma) = 3q_e B' \gamma^2 \Gamma/16 m_e c$. FC implies that $\gamma_c \ll \gamma_m$ and therefore that $\nu_c \ll \nu_m$.

The FC spectrum had so far been investigated only for $\nu_{sa} < \nu_c < \nu_m$, using a homogeneous distribution of electrons (SPN; Sari & Piran 1999), where ν_{sa} is the self-absorption frequency. Under these assumptions, the spectrum consists of four power-law segments: $F_\nu \propto \nu^2$, $\nu^{1/3}$, $\nu^{-1/2}$, and $\nu^{-p/2}$, from low to high frequencies. The spectral slope above ν_m is related to the electron injection distribution: the number of electrons with Lorentz factors $\sim\gamma$ is proportional to γ^{1-p}, and their energy is proportional to γ^{2-p}. As these electrons cool, they deposit most of their energy into a frequency range $\sim\nu_{syn}(\gamma) \propto \gamma^2$, and therefore $F_\nu \propto \gamma^{-p} \propto \nu^{-p/2}$. At $\nu_c < \nu < \nu_m$, all the electrons in the system contribute as they all cool on the dynamical time t_{dyn}. Since the energy of an electron is proportional to γ and its typical frequency is proportional to γ^2, the flux per unit frequency is proportional to $\gamma^{-1} \propto \nu^{-1/2}$. The synchrotron low-frequency tail of the cooled electrons ($\propto \nu^{1/3}$) appears at $\nu_{sa} < \nu < \nu_c$. Below ν_{sa}, the system is optically thick to self-absorption, and we see the Rayleigh-Jeans portion of the black-

[1] Racah Institute of Physics, Hebrew University, Jerusalem, 91904, Israel; jgranot@nikki.fiz.huji.ac.il, tsvi@nikki.fiz.huji.ac.il.

[2] Theoretical Astrophysics, California Institute of Technology, Pasadena, CA 91125; sari@tapir.caltech.edu.

[3] The dynamical time is the time required for considerable expansion. Adiabatic cooling is therefore negligible compared with radiative cooling.

[4] The exact shape of the electron injection distribution does not effect the optically thick part of the spectrum, which is the main concern of this work, as long as it possesses an effective low-energy cutoff at some γ_m.
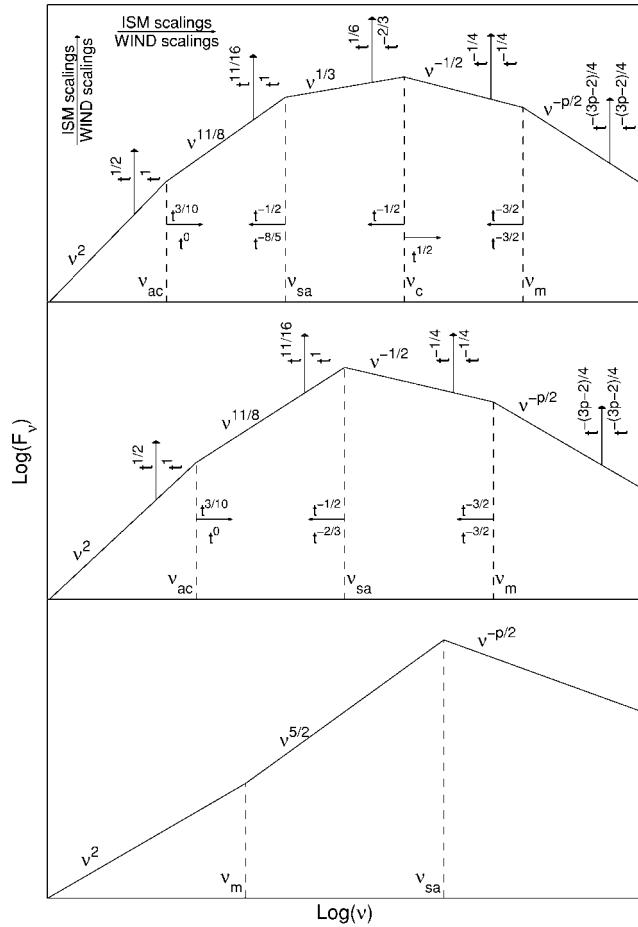
FIG. 1.—FC synchrotron spectra from a shock-injected power-law electron distribution. The shape of the spectrum is determined by the ordering of the self-absorption frequency, ν_{sa}, with respect to $\nu_c < \nu_m$. There are three possible shapes for the spectrum, corresponding to $\nu_{sa} < \nu_c$, $\nu_c < \nu_{sa} < \nu_m$, and $\nu_{sa} > \nu_m$, from top to bottom. Scalings for an afterglow, in both ISM and wind environments, are given only in the top two panels since, for typical parameters, $\nu_{sa} < \nu_m$ during the FC phase of the afterglow.

body spectrum:

$$F_\nu \propto \nu^2 \gamma_{typ}(\nu),\qquad(2)$$

where $\gamma_{typ}(\nu)$ is the typical Lorentz factor (or normalized effective temperature) of the electrons emitting at the observed frequency ν. Assuming $\gamma_{typ}(\nu) = \gamma_c \propto \nu^0$, one obtains $F_\nu \propto \nu^2$.

We derive the FC spectrum of an inhomogeneous electron temperature distribution in § 2. We find a new self-absorption regime in which $F_\nu \propto \nu^{11/8}$. In § 3, we calculate the break frequencies and flux densities for ESs (afterglows) with a spherical adiabatic evolution, both for a homogeneous external medium and for a stellar wind environment. ISs are treated in § 4. In § 5, we show that the early radio afterglow observations may be affected by the new spectra. We find that synchrotron self-absorption is unlikely to produce the steep slopes observed in some bursts in the 1–10 keV range. We also discuss the possibility of using the new spectra to probe very small scales behind the shock.

2. FAST COOLING SPECTRUM

The shape of the FC spectrum is determined by the relative ordering of ν_{sa} with respect to $\nu_c < \nu_m$. There are three possible

cases. We begin with $\nu_{sa} < \nu_c < \nu_m$, hereafter case 1. This is the "canonical" situation, which arises for a reasonable choice of parameters for afterglows in an ISM environment. The optically thin part of the spectrum ($\nu > \nu_{sa}$) of an inhomogeneous electron distribution is similar to the homogeneous one. All the photons emitted in this regime escape the system, rendering the location of the emitting electrons unimportant. In the optically thick regime ($\nu < \nu_{sa}$), most of the escaping photons are emitted at an optical depth $\tau_\nu \sim 1$, and $\gamma_{typ}(\nu)$ must be evaluated at the place where $\tau_\nu = 1$. In an ongoing shock, there is a continuous supply of newly accelerated electrons. These electrons are injected right behind the shock with Lorentz factors $\gamma \geq \gamma_m$, and then they begin to cool because of radiation losses. In the relativistic shock frame, the shocked fluid moves backward at a speed of $c/3$: $l' = ct'/3$, where l' is the distance of a fluid element behind the shock and t' is the time since it passed the shock. Just behind the shock, there is a thin layer where the electrons have not had sufficient time to cool significantly. Behind this thin layer, there is a much wider layer of cooled electrons. All these electrons have approximately the same Lorentz factor: $\gamma(t') = 6\pi m_e c/\sigma_T B'^2 t'$, or equivalently $\gamma(l') = 2\pi m_e c^2/\sigma_T B'^2 l'$. Electrons that were injected early on and have cooled down to γ_c are located at the back of the shell, at a distance of $\Delta' = ct'_{dyn}/3 = c\Gamma t_{dyn}/3 = \Gamma\Delta$ behind the shock [i.e., $\gamma_c = \gamma(\Delta') = \gamma(t'_{dyn})$]. We define the boundary between the two layers, l'_0, as the place where an electron with an initial Lorentz factor γ_m cools down to $\gamma_m/2$:

$$l'_0 = \frac{2\pi m_e c^2}{\sigma_T B'^2 \gamma_m} = \frac{3 m_e^2 c^4 n'}{4\sigma_T \epsilon_e \epsilon_B e'^2}.\qquad(3)$$

The uncooled layer is indeed very thin, as $l'_0/\Delta' = \gamma_c/\gamma_m \ll 1$. We define $l'_1(\nu)$ by $\tau_\nu(l'_1) = 1$. The optically thin emission from $l' < l'_1$ equals the optically thick emission:

$$n' l'_1 \Gamma^2 \frac{P_{\nu,\max}}{4\pi} \left\{\frac{\nu}{\nu_{syn}[\gamma(l'_1)]}\right\}^{1/3} = \left(\frac{2\nu^2}{c^2}\right) \Gamma\gamma(l'_1) m_e c^2,\qquad(4)$$

where $P_{\nu,\max} \approx P_{syn}(\gamma)/\nu_{syn}(\gamma) \propto \gamma^0$ and $P_{syn}(\gamma) = \Gamma^2 \sigma_T c \gamma^2 B'^2/6\pi$ are the peak spectral power and total synchrotron power of an electron, respectively. Since $\nu_{syn}(\gamma) \propto \gamma^2$ and, within the cooled layer, $\gamma = \gamma(l') \propto 1/l'$, equation (4) implies that $\gamma_{typ} = \gamma(l'_1) \propto \nu^{-5/8}$. We now use equation (2) and obtain that $F_\nu \propto \nu^{11/8}$. This new spectral regime is a blackbody spectrum, modified by the fact that the effective temperature (γ_{typ}) varies with frequency.

At sufficiently low frequencies, $l'_1(\nu) < l'_0$, implying $\gamma_{typ} = \gamma_m \propto \nu^0$ and $F_\nu \propto \nu^2$. The transition from absorption by the cooled electrons ($F_\nu \propto \nu^{11/8}$) to absorption by uncooled electrons ($F_\nu \propto \nu^2$) is at ν_{ac}, which satisfies $l'_1(\nu_{ac}) = l'_0$. The resulting spectrum is shown in the top panel of Figure 1; ν_{ac} may be obtained from equation (4) by substituting $\gamma(l'_1) = \gamma_m$ and $l'_1 = l'_0$ from equation (3). Substituting $\gamma(l'_1) = \gamma_c$ from equation (1) and $l'_1 = \Delta' = \Gamma\Delta$ into equation (4) gives us $\nu_{sa}^{(1)}$. The superscript "(i)" labels the specific case under consideration. We obtain

$$\nu_{ac} = \left(\frac{6 m_e^{12} c^{29} \Gamma^5 n'^{11}}{\pi^5 \epsilon_B^2 \epsilon_e^8 q_e^4 e'^{10}}\right)^{1/5},$$

$$\nu_{sa}^{(1)} = \frac{8}{3\pi}\left(\frac{4\sigma_T^8 \epsilon_B^6 \Gamma^{13} \Delta^8 n'^3 e'^6}{9 m_e^4 c^3 q_e^4}\right)^{1/5}.\qquad(5)$$

The ratio $\nu_{sa}^{(1)}/\nu_{ac} = (\gamma_m/\gamma_c)^{8/5} = (\nu_m/\nu_c)^{4/5}$ depends on the cooling rate. The maximal flux density occurs at $\nu_c = \nu_{syn}(\gamma_c)$ and is given by $F_{\nu, max}^{(1)} = N_e P_{\nu, max}/4\pi D^2$ (SPN), where N_e is the number of emitting electrons and D is the distance to the observer, while $\nu_m = \nu_{syn}(\gamma_m)$:

$$\nu_c = \frac{27\sqrt{\pi}m_e c q_e}{64\sqrt{2}\sigma_T^2 \Gamma \epsilon_B^{3/2} t_{dyn}^2 e'^{3/2}},$$

$$\nu_m = \frac{\sqrt{\pi}q_e \Gamma \epsilon_B^{1/2} \epsilon_e^2 e'^{5/2}}{12\sqrt{2}m_e^3 c^5 n'^2},$$

$$F_{\nu, max}^{(1)} = \frac{4\sqrt{2}\sigma_T m_e c^2 N_e \Gamma \epsilon_B^{1/2} e'^{1/2}}{9\pi^{3/2} q_e D^2}. \qquad (6)$$

For $\nu_c < \nu_{sa} < \nu_m$ (case 2), the cooling frequency ν_c becomes unimportant since it lies in the optically thick regime. Now there are only three transition frequencies; ν_{ac} and ν_m are similar to case 1. The peak flux $F_{\nu, max}^{(2)}$ is reached at $\nu_{sa}^{(2)}$:

$$\nu_{sa}^{(2)} = (\nu_{sa}^{(1)})^{5/9}\nu_c^{4/9},$$

$$F_{\nu, max}^{(2)} = F_{\nu, max}^{(1)}\left(\frac{\nu_c}{\nu_{sa}^{(1)}}\right)^{5/18}. \qquad (7)$$

If $\nu_c < \nu_m < \nu_{sa}$ (case 3), then $l'_1(\nu) \ll l'_0$ for $\nu < \nu_{sa}^{(3)}$. Now, both ν_{ac} and ν_c are irrelevant since the inner parts, where these frequencies are important, are not visible. We can use the initial electron distribution to estimate γ_{typ}: $\gamma_{typ} = \gamma_m \propto \nu^0$ at $\nu < \nu_m$, implying $F_\nu \propto \nu^2$. At $\nu_m < \nu < \nu_{sa}$, the emission is dominated by electrons with $\nu_{syn}(\gamma) \sim \nu$, implying $\gamma_{typ} \propto \nu^{1/2}$ and $F_\nu \propto \nu^{5/2}$. $F_{\nu, max}^{(3)}$ is reached at $\nu_{sa}^{(3)}$:

$$\nu_{sa}^{(3)} = [(\nu_{sa}^{(1)})^{10/3}\nu_c^{8/3}\nu_m^{p-1}]^{1/(p+5)},$$

$$F_{\nu, max}^{(3)} = F_{\nu, max}^{(1)}[(\nu_{sa}^{(1)})^{-p/3}\nu_c^{(3-p)/6}\nu_m^{(p-1)/2}]^{5/(p+5)}. \qquad (8)$$

It is interesting to note that the spectrum of case 3 is also valid for slow cooling (SC), that is, even if $\nu_m < \nu_c < \nu_{sa}$. This can be understood in two ways. First, as ν_c is within the optically thick regime, it is irrelevant, and hence its ordering with respect to ν_m is irrelevant. Alternatively, all the electrons contributing to this spectrum are at $l' < l'_0$, where most of the electrons have not cooled significantly and the electron distribution is the same as for SC, and hence the spectrum is the same.

Both the homogeneous spectrum, which ignores the spatial effect, and the new spectra, which are shown in Figure 1, have a low-energy tail proportional to ν^2. However, the effective temperature of the electrons is given by γ_c in the homogeneous spectrum and by γ_m in Figure 1. The new estimate of the flux density at low frequencies is therefore higher by a factor of $\gamma_m/\gamma_c = (\nu_m/\nu_c)^{1/2}$ than the previous one.

3. APPLICATION TO EXTERNAL SHOCKS AND THE AFTERGLOW

Consider now the FC spectrum of an ES that is formed when a relativistic flow decelerates as it sweeps the ambient medium. This is the leading scenario for GRB afterglow. We consider an adiabatic spherical outflow running into a cold ambient medium with a density profile $\rho(r) \propto r^{-\alpha}$, for either $\alpha = 0$ (homogeneous ISM) or $\alpha = 2$ (stellar wind environment). FC lasts for the first hour or so in a typical ISM surrounding, and for about a day in a stellar wind of a massive progenitor. The

proper number density and internal energy density behind the shock are given by the shock jump conditions: $n' = 4\Gamma n$ and $e' = 4\Gamma^2 n m_p c^2$, where n is the proper number density before the shock and m_p is the mass of a proton. We also use $\Delta = R/12\Gamma^2$, $R = 4\Gamma^2 ct$, and $t_{dyn} = t$, where t is the observed time.

For a homogeneous environment, $N_e = 4\pi n R^3/3$. Using $\Gamma \propto t^{-3/8}$ (e.g., SPN), we obtain

$$\nu_{ac} = 1.7 \times 10^9 \text{ Hz } \epsilon_{B, 0.1}^{-2/5}\epsilon_{e, 0.1}^{-8/5}E_{52}^{-1/10}n_1^{3/10}t_2^{3/10},$$

$$\nu_{sa}^{(1)} = 1.8 \times 10^{10} \text{ Hz } \epsilon_{B, 0.1}^{6/5}E_{52}^{7/10}n_1^{11/10}t_2^{-1/2},$$

$$\nu_c = 2.9 \times 10^{15} \text{ Hz } \epsilon_{B, 0.1}^{-3/2}E_{52}^{-1/2}n_1^{-1}t_2^{-1/2},$$

$$\nu_m = 5.5 \times 10^{16} \text{ Hz } \epsilon_{B, 0.1}^{1/2}\epsilon_{e, 0.1}^{2}E_{52}^{1/2}t_2^{-3/2},$$

$$F_{\nu, max}^{(1)} = 30 \text{ mJy } D_{28}^{-2}\epsilon_{B, 0.1}^{1/2}E_{52}n_1^{1/2}, \qquad (9)$$

where $n_1 = n/1 \text{ cm}^{-3}$, $E_{52} = E/10^{52}$ ergs, $D_{28} = D/10^{28}$ cm, $\epsilon_{B, 0.1} = \epsilon_B/0.1$, $\epsilon_{e, 0.1} = \epsilon_e/0.1$, and $t_2 = t/100$ s. For typical parameters, only the case 1 spectrum is expected. After $\sim$1 hr, SC sets in, and the spectrum is given in SPN.

For a circumstellar wind environment, $n = r^{-2}A/m_p$ and $N_e = 4\pi AR/m_p$. Using $\Gamma \propto t^{-1/4}$ and $A = 5 \times 10^{11}A_\star$ g cm^{-1} as in Chevalier & Li (2000), we obtain

$$\nu_{ac} = 3.6 \times 10^{10} \text{ Hz } A_\star^{3/5}\epsilon_{B, 0.1}^{-2/5}\epsilon_{e, 0.1}^{-8/5}E_{52}^{-2/5},$$

$$\nu_{sa}^{(1)} = 8.0 \times 10^{11} \text{ Hz} A_\star^{11/5}\epsilon_{B, 0.1}^{6/5}E_{52}^{-2/5}t_{hr}^{-8/5},$$

$$\nu_c = 2.5 \times 10^{12} \text{ Hz } A_\star^{-2}\epsilon_{B, 0.1}^{-3/2}E_{52}^{1/2}t_{hr}^{1/2},$$

$$\nu_m = 1.2 \times 10^{14} \text{ Hz } \epsilon_{B, 0.1}^{1/2}\epsilon_{e, 0.1}^{2}E_{52}^{1/2}t_{hr}^{-3/2},$$

$$F_{\nu, max}^{(1)} = 0.39 \text{ Jy } D_{28}^{-2}A_\star\epsilon_{B, 0.1}^{1/2}E_{52}^{1/2}t_{hr}^{-1/2},$$

$$\nu_{sa}^{(2)} = 1.3 \times 10^{12} \text{ Hz } A_\star^{1/3}t_{hr}^{-2/3},$$

$$F_{\nu, max}^{(2)} = 0.54 \text{ Jy } D_{28}^{-2}A_\star^{-1/6}\epsilon_{B, 0.1}^{-1/4}E_{52}^{3/4}t_{hr}^{1/12}, \qquad (10)$$

where $t_{hr} = t/1$ hr. For typical parameters, the spectrum is of case 2 for $\sim$1–2 hr after the burst. Then it turns to case 1 until $\sim$1 day, when there is a transition to SC. The SC spectrum is given in Chevalier & Li (2000).

4. APPLICATION TO INTERNAL SHOCKS AND THE GRB

ISs are believed to produce the GRBs themselves. The temporal variability of the bursts is attributed to emission from many different collisions between shells within the flow. The number of peaks in a burst, N, roughly corresponds to the number of such shells. Different shells typically collide before their initial width, Δ_i, has expanded significantly. Assuming that the typical initial separation between shells is $\sim\Delta_i$, $\Delta_i = cT_{90}/2N$ on average, where T_{90} is the duration of the burst. The average energy of a shell is $E_{sh} \approx E/N$, where E is the total energy of the relativistic flow. The emission in the optically thick regime comes from the shocked fluid of the outer and slower shells. We denote the initial Lorentz factor of this shell by Γ_i and its Lorentz factor after the passage of the shock by Γ. The average thermal Lorentz factor of the protons in this region equals the relative bulk Lorentz factor of the shocked and unshocked portions of the outer shell, $\Gamma_r = \Gamma/2\Gamma_i$, which is typically of order unity. Therefore, $e' = \Gamma_r n' m_p c^2$. One can estimate the number density of the preshocked fluid n'_i by the number of electrons in the shell, $N_e = E_{sh}/\Gamma_i m_p c^2$, divided by its volume: $n'_i = N_e/4\pi R^2 \Delta_i \Gamma_i$. The number density of the

shocked fluid, which is the one relevant for our calculations, is $n' = 4\Gamma_r n_i'$. The width of the front shell in the observer frame decreases after it is shocked: $\Delta = \Delta_i/8\Gamma_r^2$. In this section, we use $R \sim 2\Gamma_i^2 \Delta_i \sim 4\Gamma^2 \Delta$, which is the typical radius for collision between shells, and $t_{\mathrm{dyn}} \sim 3\Delta/c$. Thus, we obtain

$$\nu_{\mathrm{ac}} = 8.7 \times 10^{14} \mathrm{\ Hz\ } \Gamma_{r,3}^{-3/5} \epsilon_{B,0.1}^{-2/5} \epsilon_{e,0.1}^{-8/5} E_{52}^{1/5} \Gamma_3^{-1/5} N_2^{2/5} T_1^{-3/5},$$

$$\nu_{\mathrm{sa}}^{(1)} = 7.7 \times 10^{19} \mathrm{\ Hz\ } \Gamma_{r,3}^{53/5} \epsilon_{B,0.1}^{6/5} E_{52}^{9/5} \Gamma_3^{-41/5} N_2^{2} T_1^{-19/5},$$

$$\nu_c = 3.6 \times 10^{12} \mathrm{\ Hz\ } \Gamma_{r,3}^{-8} \epsilon_{B,0.1}^{-3/2} E_{52}^{-3/2} \Gamma_3^{8} N_2^{-1} T_1^{5/2},$$

$$\nu_m = 5.6 \times 10^{18} \mathrm{\ Hz\ } \Gamma_{r,3}^{6} \epsilon_{B,0.1}^{1/2} \epsilon_{e,0.1}^{2} E_{52}^{1/2} \Gamma_3^{-2} N_2 T_1^{-3/2},$$

$$F_{\nu,\mathrm{max}}^{(1)} = 509 \mathrm{\ Jy\ } \Gamma_{r,3}^{5} \epsilon_{B,0.1}^{1/2} E_{52}^{3/2} \Gamma_3^{-3} D_{28}^{-2} T_1^{-3/2},$$

$$\nu_{\mathrm{sa}}^{(2)} = 4.3 \times 10^{16} \mathrm{\ Hz\ } \Gamma_{r,3}^{7/3} E_{52}^{1/3} \Gamma_3^{-1} N_2^{2/3} T_1^{-1}, \qquad (11)$$

where $N_2 = N/100$, $T_1 = T_{90}/10$ s, $\Gamma_{r,3} = \Gamma_r/3$, and $\Gamma_3 = \Gamma/10^3$.

5. DISCUSSION

We have calculated the synchrotron spectrum of FC electrons. We find three possible spectra, depending on the relative ordering of ν_{sa} with respect to $\nu_c < \nu_m$. Two of these spectra contain a new self-absorption regime in which $F_\nu \propto \nu^{11/8}$.

During the initial FC stage of the afterglow, the system is typically optically thick in the radio and optically thin in the optical and X-ray, for both ISM and stellar wind environments. We therefore expect the new feature, $F_\nu \propto \nu^{11/8}$, to be observable only in the radio band, during the afterglow. For both environments, ν_{ac} and ν_{sa} move closer together (see Fig. 1), until they merge at the transition to SC. Afterward, there is only one self-absorption break, at $\nu_{\mathrm{sa}}^{(SC)}$.

For an ISM surrounding, $\nu_{\mathrm{sa}}^{(SC)} \propto t^0$ (as long as $\nu_{\mathrm{sa}} < \nu_m$). From current late-time radio observations, we know that typically, $\nu_{\mathrm{sa}}^{(SC)} \sim$ a few GHz (Taylor et al. 1998; Wijers & Galama 1999; Granot, Piran, & Sari 1999b). Therefore, the whole VLA band, 1.4–15 GHz, should initially be in the range where $F_\nu \propto \nu^{11/8}$. Sufficiently early radio observations, which could confirm this new spectral slope, may become available in the upcoming *High-Energy Transient Explorer* era.

In a considerable fraction of bursts, there is evidence for a spectral slope greater than 1/3 (photon number slope greater than $-2/3$) in the 1–10 keV range (Preece et al. 1998; Crider

et al. 1997; Strohmayer et al. 1998). Such spectral slopes are not possible for optically thin synchrotron emission (Katz 1994). They could be explained by self-absorbed synchrotron emission if ν_{sa} reaches the X-ray band. The best prospects for this to occur are with the spectrum of the second type. However, we have to check whether the physical parameters for which ν_{sa} is so high are reasonable. Several constraints must be satisfied: (1) ISs must occur at smaller radii than ESs, (2) efficient emission requires FC, and (3) the system must be optically thin to Thomson scattering and pair production. The most severe constraint in the way of getting the ν_{sa} into the X-ray band arises from the third constraint. It is possible only for rather extreme parameters: $\Gamma \sim 10^4$ and $\Gamma_r \sim 50$. With such parameters, νF_ν would peak at $h\nu_m \sim 1$–100 GeV, unless $\epsilon_e \lesssim 10^{-2}$, which would result in a very low radiative efficiency. Overall, it seems unlikely that self-absorbed synchrotron emission produces the observed spectral slopes greater than 1/3.

So far, we have neglected inverse Compton scattering (IC). For $\epsilon_e < \epsilon_B$, the effects of IC are small since the total power, P_{IC}, emitted via IC is smaller than via synchrotron emission: $P_{\mathrm{IC}} < P_{\mathrm{syn}}$. For $\epsilon_e > \epsilon_B$, IC becomes important as $P_{\mathrm{IC}}/P_{\mathrm{syn}} = (\epsilon_e/\epsilon_B)^{1/2}$ (Sari et al. 1996). This additional cooling causes γ_c and ν_c to decrease by factors of $(\epsilon_e/\epsilon_B)^{1/2}$ and ϵ_e/ϵ_B, respectively. This increases the duration of the FC stage in ESs by factors of ϵ_e/ϵ_B and $(\epsilon_e/\epsilon_B)^{1/2}$ for ISM and stellar wind environments, respectively.

Our results depend on the assumption of an orderly layered structure behind the shock: a thin uncooled layer of width l_0', followed by a much wider layer of cooled electrons of width $\Delta' = l_0' (\nu_m/\nu_c)^{1/2}$. Clearly, significant mixing would homogenize the region and would lead to the "homogeneous" spectrum given in SPN, without the $\nu^{11/8}$ region discussed here. A typical electron is not expected to travel much farther than its gyration radius, $r(\gamma)$. We obtain $r(\gamma_m)/l_0' = 5 \times 10^{-8} t_2^{-9/8}$, $10^{-9} t_{\mathrm{hr}}^{-5/4}$, and 5×10^{-8} using the scalings of equations (9) and (10) for ESs and equation (11) for ISs, respectively. Thus, this effect could not cause significant mixing. Another mechanism that might cause mixing is turbulence. The observation of a spectrum with $F_\nu \propto \nu^{11/8}$ would indicate the existence of a layered structure and would constrain the effective mixing length to $\lesssim l_0' = \Delta' (\nu_c/\nu_m)^{1/2}$.

REFERENCES

Chevalier, R. A., & Li, Z.-Y. 2000, ApJ, in press (astro-ph/9908272)
Crider, A., et al. 1997, ApJ, 479, L39
Fenimore, E., et al. 1996, ApJ, 473, 998
Granot, J., Piran, T., & Sari, R. 1999a, ApJ, 513, 679
———. 1999b, ApJ, 527, 236
Katz, J. 1994, ApJ, 432, L107
Katz, J., & Piran, T. 1997, ApJ, 490, 772
Mészáros, P., & Rees, M. 1997, ApJ, 476, 232
Preece, R. D., et al. 1998, ApJ, 506, L23

Sari, R., Narayan, R., & Piran, T. 1996, ApJ, 473, 204
Sari, R., & Piran, T. 1997, ApJ, 485, 270
———. 1999, ApJ, 520, 641
Sari, R., Piran, T., & Narayan, R. 1998, ApJ, 497, L17 (SPN)
Strohmayer, T. E., et al. 1998, ApJ, 500, 873
Taylor, G. B., et al. 1998, ApJ, 502, L115
Waxman, E. 1997, ApJ, 485, L5
Wijers, R. A. M. J., & Galama, T. J. 1999, ApJ, 523, 177